Neurobiology of Disease

D_2-Like Receptor Expression in the Hippocampus and Amygdala Informs Performance on the Stop-Signal Task in Parkinson's Disease

Leah G. Mann,[1,2] Kaitlyn R. Hay,[2] Alexander K. Song,[2] Steven P. Errington,[3] Paula Trujillo,[2] David H. Zald,[3,4] Yan Yan,[5] Hakmook Kang,[5] Gordon D. Logan,[3] and Daniel O. Claassen[2]

[1]Vanderbilt Brain Institute, Vanderbilt University, Nashville, Tennessee 37232, [2]Department of Neurology, Vanderbilt University Medical Center, Nashville, Tennessee 37232, [3]Department of Psychology, Vanderbilt University, Nashville, Tennessee 37240, [4]Department of Psychiatry, Rutgers University, Piscataway, New Jersey 08854, and [5]Department of Biostatistics, Vanderbilt University Medical Center, Nashville, Tennessee 37203

The stop-signal task is a well-established assessment of response inhibition, and in humans, proficiency is linked to dorsal striatum D_2 receptor availability. Parkinson's disease (PD) is characterized by changes to efficiency of response inhibition. Here, we studied 17 PD patients (6 female and 11 male) using the stop-signal paradigm in a single-blinded D-amphetamine (dAMPH) study. Participants completed [^{18}F]fallypride positron emission topography (PET) imaging in both placebo and dAMPH conditions. A voxel-wise analysis of the relationship between binding potential (BP_{ND}) and stop-signal reaction time (SSRT) revealed that faster SSRT is associated with greater D_2-like BP_{ND} in the amygdala and hippocampus (right cluster $q_{FDR\text{-}corr} = 0.026$, left cluster $q_{FDR\text{-}corr} = 0.002$). A region of interest (ROI) examination confirmed this association in both the amygdala (coefficient = −48.26, $p = 0.005$) and hippocampus (coefficient = −104.94, $p = 0.007$). As healthy dopaminergic systems in the dorsal striatum appear to regulate response inhibition, we interpret our findings in PD to indicate either nigrostriatal damage unmasking a mesolimbic contribution to response inhibition, or a compensatory adaptation from the limbic and mesial temporal dopamine systems. These novel results expand the conceptualization of action-control networks, whereby limbic and motor loops may be functionally connected.

Key words: **dopamine; hippocampus; limbic; mesial temporal; Parkinson's disease; response inhibition**

Significance Statement

While Parkinson's disease (PD) is characteristically recognized for its motor symptoms, some patients develop impulsive and compulsive behaviors (ICBs), manifested as repetitive and excessive participation in reward-driven activities, including sex, gambling, shopping, eating, and hobbyism. Such cognitive alterations compel a consideration of response inhibition in PD. To investigate inhibitory control and assess the brain regions that may participate, we assessed PD patients using a single-blinded D-amphetamine (dAMPH) study, with [^{18}F]fallypride positron emission topography (PET) imaging, and stop-signal task performance. We find a negative relationship between D_2-like binding in the mesial temporal region and top-signal reaction time (SSRT), with greater BP_{ND} associated with a faster SSRT. These discoveries indicate a novel role for mesolimbic dopamine in response inhibition, and advocate for limbic regulation of action control in this clinical population.

Introduction

Parkinson's disease (PD) is a neurodegenerative disorder characterized by dopaminergic and monoaminergic neuronal loss. Although motor symptoms respond to dopamine therapy, nonmotor symptoms are more variable and arise as greater sources of clinical burden to patients (Martinez-Martin et al., 2011). Impulsivity is one well-described clinical phenomenon in PD, whereby some patients develop impulsive and compulsive behaviors (ICBs; Weintraub et al., 2010), and others experience motor impulsiveness that contributes to falls (Ahlskog, 2010).

While generally understood as an inability to suppress an impetuous drive, a unitary definition must be eschewed, and

Received May 6, 2021; revised Sep. 23, 2021; accepted Oct. 25, 2021.

Author contributions: D.H.Z. and D.O.C. designed research; K.R.H., A.K.S., and P.T. performed research; L.G.M., A.K.S., S.P.E., P.T., Y.Y., H.K., G.D.L., and D.O.C. analyzed data; L.G.M. wrote the first draft of the paper; L.G.M., S.P.E., P.T., D.H.Z., G.D.L., and D.O.C. edited the paper; L.G.M. wrote the paper.

This work was supported by the National Institute on Aging Grant 1K24AG064114 (to D.O.C.) and the National Institute of Neurological Disorders and Stroke Grant 5R01NS097783 (to D.O.C.).

The authors declare no competing financial interests.

Correspondence should be addressed to Daniel O. Claassen at daniel.claassen@vumc.org.

https://doi.org/10.1523/JNEUROSCI.0968-21.2021

impulsivity must instead be recognized as a multifaceted cognitive process (Bechara et al., 2000). Two common distinctions are cognitive impulsivity, which is grounded in reward-based decision-making, and motor impulsivity, which focuses on response inhibition (Bechara et al., 2000). Cognitive neuroscience paradigms that assess action control can be conceptually linked to interpretations of motor impulsivity. One such tool is the stop-signal task, which serves as the benchmark for measuring response inhibition. The paradigm involves participants making speeded choice reactions to "go" stimuli, and occasionally inhibiting their reactions on the occurrence of a "stop" signal (Logan and Cowan, 1984). The task assesses the stop-signal reaction time (SSRT), or the speed with which one cancels the preparation of an already initiated response.

Although the range of neuromodulatory systems associated with stop-signal task performance is not fully elucidated, dopamine has been considered a significant contributor to action control (Mink, 1996). Studies of clinical populations suffering from dopaminergic dysfunction have demonstrated slower inhibitory processes with longer SSRTs (Colzato et al., 2007; Enticott et al., 2008). Moreover, reduced spontaneous eyeblink rate, an index of dopaminergic function, is correlated with slower SSRT (Colzato et al., 2009). In rodents, the role of dopaminergic activity on SSRT has been recognized in the dorsomedial striatum, with D_2-specific blockade increasing SSRT (Eagle et al., 2011). Similarly, correlations between D_2 binding potential (BP_{ND}) and SSRT have been localized to the caudate and putamen in healthy humans (Ghahremani et al., 2012; Robertson et al., 2015).

Poor response inhibition often accompanies psychiatric disorders that manifest with impulsivity (Moeller et al., 2001). However, in PD patients with ICBs, action control is maintained, such that they demonstrate faster SSRTs than either healthy controls or PD patients without ICBs (Claassen et al., 2015). Self-reported measures disclose that ICB patients present with increased cognitive, but not motor, impulsivity on the Barret Impulsivity Scale-11 (BIS-11; Aumann et al., 2020). The preservation or even enhancement of inhibitory motor control in ICB patients suggests key distinctions in the pattern of dopamine alterations among PD patients. Such a possibility is consistent with current evidence for differences to mesocorticolimbic dopamine regulation in ICB patients, with strengthened network connectivity, reduced D_2-like BP_{ND} in the ventral striatum and putamen, and low dopamine tone in the anterior cingulate cortex (Ray et al., 2012; Petersen et al., 2018; Stark et al., 2018a). Additionally, following administration of dopamine agonist medication, PD patients have shown increased regional cerebral blood flow in the dorsolateral prefrontal cortex, accompanied by improved inhibitory control (Trujillo et al., 2019). Motor inhibition in PD patients may involve mesolimbic networks because of the predominant damage of dopaminergic innervation in the striatum.

In this study, we tested the hypothesis that D_2-mediated striatal and extrastriatal networks may function as a compensatory system for facilitating inhibitory control in PD through an examination of SSRT values and D_2-like BP_{ND}. To measure baseline ability and sensitivity to modulation by dopamine release, PD patients, with and without ICBs, completed the stop-signal task following placebo and D-amphetamine (dAMPH) administration. To determine the association of different brain regions, participants also underwent two positron emission topography (PET) imaging scans with [^{18}F]fallypride, a high affinity $D_{2/3}$ receptor ligand, under placebo and dAMPH. This assessment was performed in a single-blinded fashion. Given the proficiency of SSRT performance in PD-ICB patients, we hypothesized that ventral striatal D_2 BP_{ND} would be associated with faster SSRT and that dAMPH administration would improve performance.

Materials and Methods

Participants

All PD patients ($n = 17$, sex = 6 female/11 male) were recruited from the Movement Disorders Clinic at Vanderbilt University Medical Center. Patients met United Kingdom Brain Bank criteria for idiopathic PD (Hughes et al., 1992) and were diagnosed by a movement disorder neurologist (D.O.C.). All patients were screened to confirm that they met inclusion criteria, and further did not have an implanted deep brain stimulator, an unstable medical condition, a comorbid neurologic disorder, dementia, a history of major psychiatric illness, or a history of substance abuse. Additionally, no patients had taken psychostimulants over the previous year, and were not currently using cocaine, nicotine or excessive alcohol. The majority of participants were taking DA agonist medications along with concomitant levodopa therapy. Dopamine medications were converted to levodopa equivalent dose (LEDD; Tomlinson et al., 2010). The study was conducted in accordance with the Declaration of Helsinki, and all subjects provided written, informed consent before participating in the study in compliance with the standards of ethical conduct in human investigation regulated by the local Institutional Review Board.

Along with a physical examination, neurologic examination, EKG, urinalysis, and metabolic panel, a set of questionnaires was also administered during study screening. Patients completed part II of the Movement Disorders Society-United Parkinson's Disease Rating Scale (MDS-UPDRS), which serves as a self-evaluation of motor activities of daily living, and part III (in the Off-medication condition), which serves as a clinician-scored motor examination (Goetz et al., 2008; Weintraub et al., 2012). Symptoms of depression were assessed using the Center for Epidemiologic Studies Depression Scale Revised (CESD-R). Finally, the Questionnaire for Impulsive-Compulsive Disorders in Parkinson's Disease-Rating Scale (QUIP-RS) was conducted to screen for ICBs. To define the clinical presence of ICBs, formal interviews with patients and caregivers were performed, with an ICB designation based on previously described DSM-5 criteria (Voon et al., 2006). Table 1 presents demographic and clinical information.

Participants attended two testing visits while off dopaminergic therapies. The sessions were conducted within approximately one week of each other. Before each session, participants completed a 36-h withdrawal from dopamine agonist therapy and a 16-h withdrawal from levodopa therapy, and resumed medication following the completion of the imaging study. This period was considered sufficient to eliminate effects from dopaminergic therapies, while minimizing potential patient discomfort. During the first session, participants were administered oral placebo, and in the second, they were administered a 0.43 mg/kg oral dose of dAMPH. The order of these visits was blinded to the participant only (i.e., single blind).

Stop-signal task

Approximately 30 min after medication (placebo or dAMPH) administration, but before [^{18}F]fallypride injection, patients performed a manual version of the stop-signal task (Logan and Cowan, 1984). Participants, wearing corrective lenses if prescribed, were seated at a comfortable distance from a laptop screen and provided with directions before proceeding. On Go trials, which comprised 75% of the trials, patients were presented with a fixation point followed by a left-pointing or right-pointing gray arrow in the center of the screen. They were instructed to make a left-hand button press with external response grips when they observed a left-pointing arrow and to make a right-hand button press when they observed a right-pointing arrow. Responses were to be made as quickly and accurately as possible. The time it took for a participant to press the response button following the appearance of the target was recorded as go reaction time (GoRT). Once a choice had been executed or 1200 ms had passed, the gray arrow disappeared. Next, an

Table 1. Demographic and clinical evaluation of the PD participants

Variables	All PD patients	ICB patients	Non-ICB patients	*p* value
N	17	8	9	–
Sex (M/F)	11/6	4/4	7/2	0.231[a]
Age (years)	64.2 ± 6	62.4 ± 4.5	65.8 ± 7	0.330[b]
Disease duration (years)	5.8 ± 3.5	5.7 ± 3.3	5.9 ± 3.8	0.689[b]
CES-D	15.3 ± 10.7	16.9 ± 6.9	14.1 ± 13.2	0.182[b]
MDS-UPDRS-II	13.6 ± 9.2	17.3 ± 9.6	10.4 ± 8.1	0.197[b]
MDS-UPDRS-III (off)	28.8 ± 12.5	28.4 ± 13.7	29.1 ± 12.1	0.833[b]
Total LEDD (mg/d)	680.6 ± 310	688.1 ± 315.4	673.9 ± 324.1	0.986[b]
Agonist single dose equivalent (mg/d)	75.3 ± 31.5	79.3 ± 32.5	72.2 ± 32.3	0.620[b]
QUIP-RS	23.6 ± 13.3	29.8 ± 13.2	18.1 ± 11.3	0.108[b]

Data are shown as mean ± SD.
CES-D: Center for Epidemiologic Studies Depression Scale.
MDS-UPDRS: Movement Disorders Society-United Parkinson's Disease Rating Scale.
LEDD: levodopa equivalent daily dose.
QUIP-RS: Questionnaire for Impulsive-Compulsive Disorders in Parkinson's Disease-Rating Scale.
[a] *p* value from χ^2 test between ICB and non-ICB patients.
[b] *p* value from Wilcoxon rank-sum test between ICB and non-ICB patients.

interstimulus interval between 1250 and 1750 ms occurred while the fixation point remained visible.

On Stop trials, which comprised 25% of the trials, the gray arrow changed to a purple arrow soon after appearing on the screen. Patients were instructed to attempt to restrain themselves from pressing a button after perceiving the purple arrow. The stop-signal delay, or the time between the presentation of the gray arrow and its color change was systematically regulated with a staircase design that adjusts according to the participant's performance (Levitt, 1971). Beginning at 200 ms, the delay was thereafter tuned incrementally by 50 ms, increasing if stopping was successful and decreasing if stopping was unsuccessful. In situations when stopping was unsuccessful and the participant responded, the time it took for a participant to press the button following the appearance of the target was noted as the signal-respond reaction time. Each administration of the stop-signal task involved 48 practice trials, followed by two blocks of 104 experimental trials.

Estimating SSRT

A parametric model of the stop-signal task was applied, with model parameters calculated using the Bayesian Estimation of ex-Gaussian Stop-Signal Reaction Time Distribution (BEESTS) software (Matzke et al., 2013). Reaction times that were less than or greater than three standard deviations away from the mean were removed from the analysis during preprocessing. Similar to the traditional mean and integration approaches for analyzing stop-signal task data, this model assumes that the distribution of signal-respond reaction times, or reaction times on failed stop trials, can be considered as a censored GoRT distribution. BEESTS fits the data according to an ex-Gaussian distribution, outputting μ as the mean of the Gaussian component, σ as the standard deviation of the Gaussian component, and τ as the mean and standard deviation of the exponential component for both GoRT and SSRT distributions (Matzke et al., 2013). Mean GoRT and SSRT can then be calculated as the sum of μ and τ. This method also provides an estimation of the probability of trigger failures, which represents an inability to initiate the stop process (Matzke et al., 2017). The model was run for 20,000 samples with a thinning of 5. GoRT and SSRT served as the primary assessments, representing response initiation and inhibitory control, respectively.

PET imaging protocol

[^{18}F]fallypride was synthesized in the radiochemistry core as outlined in a previously described method (Stark et al., 2018b). Data were collected on a Philips Vereos PET/CT scanner with a three-dimensional acquisition and transmission attenuation correction. Approximately 2 h after medication (placebo or dAMPH) administration, serial PET scans were acquired simultaneously with a 5.0 mCi bolus injection of [^{18}F]fallypride over a 30-s period. Scan time ran to ~3.5 h after injection with two breaks of 15 min between emission scans (Stark et al., 2018b).

Magnetic resonance imaging (MRI) protocol

Anatomical T1-weighted MR images were acquired to allow region definition for region of interest (ROI) analysis and spatial normalization for voxel-wise analyses. All MRI scans were completed with a 3.0T Philips MRI scanner with a body coil transmission and 32-channel SENSE array reception. Structural images were acquired using a T1-weighted high-resolution anatomic scan (MPRAGE; spatial resolution 1 × 1 × 1 mm^3; TR/TE = 8.9/4.6 ms).

PET image processing

[^{18}F]fallypride non-displaceable binding potential (BP_{ND}) was quantified following motion-correction with Statistical Parametric Mapping software (SPM12; Wellcome Trust Center for Neuroimaging, London, United Kingdom; https://www.fil.ion.ucl.ac.uk/spm/software/). Parametric BP_{ND} images were estimated using the simplified reference tissue model in PMOD software (PMOD Technologies; Stark et al., 2018b). The cerebellum was used as a reference region because of its limited $D_{2/3}$ receptor expression (Camps et al., 1989). Parametric BP_{ND} images were co-registered to the participant's T1-weighted MR image using FSL's FLIRT with 6 degrees of freedom and a mutual information cost function (FSL v6.0; FMRIB). For voxel-level analyses, parametric BP_{ND} images were non-linearly registered to standard Montreal Neurologic Institute (MNI152) space using FSL's FNIRT.

ROI analyses

A priori bilateral subcortical ROIs were manually defined on each participant's T1 MRI image according to established anatomic definitions (Stark et al., 2018b). These ROIs included the caudate (head), putamen, globus pallidus, ventral striatum, substantia nigra, amygdala, and cerebellum. Additionally, the hypothalamus and ventromedial orbitofrontal cortex were manually defined according to a previously described method and proposed anatomic landmarks, respectively (Mackey and Petrides, 2009; Klomp et al., 2012). The hippocampus and thalamus were segmented with FSL FIRST, and the anterior cingulate cortex and insula with FreeSurfer (v6.0; Martinos Center for Biomedical Imaging, Charlestown, MA; https://surfer.nmr.mgh.harvard.edu/fswiki).

Experimental design and statistical analyses

First, GoRT and SSRT data from the placebo and dAMPH sessions of PD patients were compared using the Wilcoxon signed-rank test. A Wilcoxon rank-sum test was used to compare the GoRT and SSRT placebo data between ICB and non-ICB patients.

To investigate the relationship between [^{18}F]fallypride BP_{ND} and stop-signal task performance, a voxel-wise analysis was completed using SPM12. The regression of $D_{2/3}$ BP_{ND} on SSRT across cortical and subcortical areas included age and sex as covariates (Mukherjee et al., 2002; Pohjalainen et al., 1998). Significance criteria consisted of an uncorrected $p < 0.005$ and cluster-level false discovery rate (FDR) controlled at 0.05 to correct for multiple comparisons. A general linear regression model

(GLM) was applied to further explore the correlation between [^{18}F]fallypride BP_{ND} and SSRT in striatal and extrastriatal ROIs. For this model, SSRT served as the dependent variable, mean ROI BP_{ND} as the independent variable, and age and sex as covariates. An FDR of 0.05 was used to correct for multiple comparisons (Benjamini and Hochberg, 1995).

An additional GLM was used to test the hypothesis that $D_{2/3}$ receptor expression in the significant regions from the first GLM may also play a role in disparate effects of dAMPH on stop-signal task performance. For this analysis, change in SSRT between placebo and dAMPH sessions served as the dependent variable, mean ROI BP_{ND} as the independent variable, and age and sex as covariates. Again, an FDR of 0.05 was used to correct for multiple comparisons. All statistical analyses were performed using R (R Foundation for Statistical Computing, Vienna, 2016).

Results

Inhibitory control performance

In order to evaluate SSRT, it is necessary to ensure that (1) the probability of failing to inhibit a response is greater at longer stop-signal delays, and (2) mean signal-respond reaction time is faster than mean GoRT. These criteria were met, validating the independent race model and the reliability of the estimates of SSRT across participants. Table 2 summarizes the behavioral results estimated by BEESTS.

SSRT following dAMPH administration data from four participants were excluded from analyses because of technological issues during task completion. Across PD patients ($n = 13$), SSRT did not significantly vary between placebo administration and dAMPH administration (placebo: 274.09 ± 36.48 ms; dAMPH: 274.47 ± 28.57 ms; $z = -0.135$, $p = 0.893$). GoRT also did not vary between drug administration conditions (placebo: 613.70 ± 113.29 ms; dAMPH: 568.37 ± 98.58 ms; $z = 0.955$, $p = 0.340$). Although patients with ICBs ($n = 8$) displayed faster SSRTs than those without ($n = 9$), the difference is not statistically significant (ICB: 260.84 ± 34.05 ms; non-ICB: 285.39 ± 33.62 ms; $z = -1.381$, $p = 0.167$). Finally, placebo GoRT also did not significantly differ between patients with ICBs and those without (ICB: 604.86 ± 134.90 ms; non-ICB: 594.91 ± 80.72 ms; $z = -0.140$, $p = 0.888$). Group level comparisons for placebo SSRT are presented in Figure 1.

Table 2. Stop-signal task performance following placebo administration

	All PD patients ($n = 17$)	ICB patients	Non-ICB patients	p value
SSRT (ms)	273.84 ± 35.10	260.84 ± 34.05	285.39 ± 33.62	0.167
GoRT (ms)	599.59 ± 106.04	604.86 ± 134.90	594.91 ± 80.72	0.888
Trigger failures (percentage)	5.67 ± 8.73	5.44 ± 10.09	5.86 ± 7.95	0.384

Data are shown as mean ± SD.
p values from Wilcoxon rank-sum test between ICB and non-ICB patients.

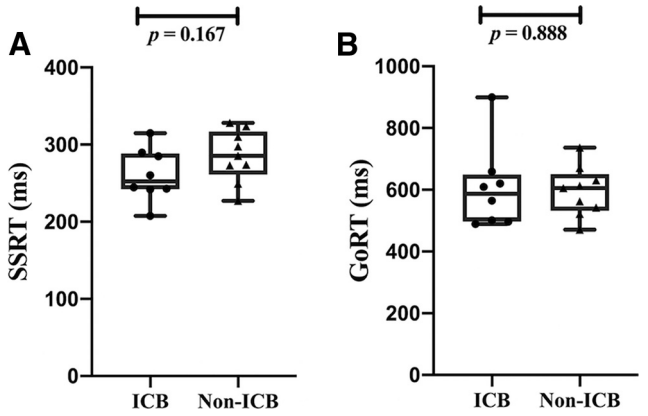

Figure 1. Group results for the stop-signal task variables. ***A***, Placebo SSRT did not significantly differ between patients with ICBs and patients without ICBs. ***B***, Placebo GoRT did not significantly differ between patients with ICBs and patients without ICBs.

Voxel-wise analysis of relationship between baseline [^{18}F] fallypride BP_{ND} and placebo SSRT

Applying the voxel-wise method with age and sex as covariates resulted in negative correlations between baseline [^{18}F]fallypride BP_{ND} and placebo SSRT in striatal and extrastriatal regions. These clusters localized to the left orbitofrontal cortex and bilaterally to the amygdala and hippocampus, surviving cluster-level FDR correction at 0.05. A cluster localized to the left caudate also emerged but was not statistically significant at cluster-level FDR correction at 0.05. Figure 2 shows a map of significant clusters overlaid on coronal and axial slices of a standard-space brain, along with coordinate and statistical information for the significant clusters. No significant clusters emerged when testing for an association between baseline [^{18}F]fallypride BP_{ND} and GoRT.

ROI-based analysis of relationship between baseline [^{18}F] fallypride BP_{ND} and placebo SSRT

Significant negative correlations between baseline [^{18}F]fallypride BP_{ND} and placebo SSRT were found in ROIs, including the amygdala (coefficient = −48.26, $p = 0.005$) and hippocampus (coefficient = −104.94, $p = 0.007$). Both the amygdala and hippocampus survived FDR correction for multiple comparisons at 0.05 ($p_{corrected} = 0.039$, $p_{corrected} = 0.039$). Figure 3 displays the significant relationships between [^{18}F]fallypride BP_{ND} and SSRT. Table 3 presents mean regional [^{18}F]fallypride BP_{ND} values for all ROIs, along with the coefficient and p values from the GLM analysis.

ROI-based analysis of relationship between baseline [^{18}F] fallypride BP_{ND} and SSRT change in response to dAMPH

The ROIs of the hippocampus and amygdala were included in this GLM. While the p values ($p = 0.075$) were not significant, the data support a negative correlation between baseline hippocampus D_2-like receptor binding, and dAMPH effects on SSRT (95% CI = [−205.987, −2.867]). Figure 4 displays this relationship between [^{18}F]fallypride BP_{ND} in the hippocampus and SSRT change.

Discussion

This study investigated the neural correlates of inhibitory control in persons with PD. As in our past work (Claassen et al., 2015), analysis of SSRT makes evident that ICB patients do not possess a deficit in stopping speed, and indeed appeared slightly faster than patients without ICBs (although this difference was not significant in this small sample). It seems increasingly apparent that motor control is not a primary contributor to ICBs in PD, and other impulsive-compulsive processes are likely more central to these deficits. An analysis of task performance in relation to dopamine receptor availability across all participants established a negative correlation in the amygdala and hippocampus, such that greater D_2-like BP_{ND} is associated with better stopping control.

A

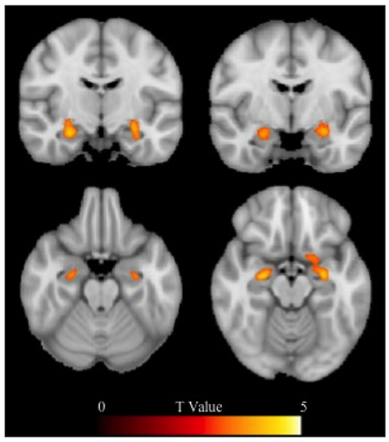

B

Regions Included in Cluster	Peak Coordinates (mm)			Cluster Size	$q_{FDR\text{-}corr}$ [a]
	x	*y*	*z*		
R Hippocampus and Amygdala	27	-11	-19	1151	0.026
L Hippocampus, Amygdala, and Orbitofrontal Cortex	-27	-8	-15	2255	0.002

[a] Significant at FDR=0.05

Figure 2. Voxel-wise regression of baseline [^{18}F]fallypride BP_{ND} on placebo SSRT. ***A***, Map of significant clusters where SSRT was negatively correlated with [^{18}F]fallypride BP_{ND} in PD patients, overlaid on coronal and axial slices of an MNI template brain. All survived cluster-level FDR correction at $p < 0.05$. Areas include the amygdala, hippocampus, and left orbitofrontal cortex. Brains are displayed according to radiologic convention, with the left side of the brain shown on the right side of the image. ***B***, Regions showing significance for a negative correlation between [^{18}F]fallypride BP_{ND} and SSRT.

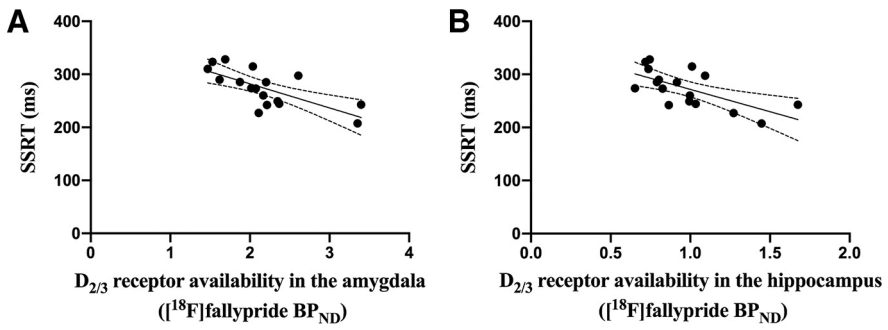

Figure 3. Scatterplots with lines of best fit displaying the relationship between placebo SSRT and baseline [^{18}F]fallypride BP_{ND}. A GLM was applied with SSRT as the dependent variable and mean ROI BP_{ND} as the independent variable. Age and sex served as covariates. A significant negative correlation between BP_{ND} and SSRT was observed for the (***A***) amygdala ($p = 0.005$) and (***B***) hippocampus ($p = 0.007$), indicating a negative relationship between $D_{2/3}$ expression and stopping control in these limbic areas.

Novel relationships between BP_{ND} in the hippocampus, amygdala, and SSRT

While previous studies have identified a negative correlation between SSRT and D_2-like BP_{ND} in the dorsal, but not ventral, striatum in healthy subjects (Ghahremani et al., 2012; Robertson et al., 2015), this study is the first to specifically examine this association in persons with PD. Interestingly, with this clinical population, a different relationship emerges, as the most robust associations emerged bilaterally in the amygdala and hippocampus of the voxel-wise and ROI-based analyses.

The manifestation of a role for limbic areas in inhibitory control in PD patients may be explained by preservation of ventral striatal and mesolimbic dopamine networks in PD. The dorsal striatum, with input from the substantia nigra, suffers a substantial loss of dopaminergic innervation early in the disease and throughout its progression (Damier et al., 1999; Björklund and Dunnett, 2007). On the other hand, while the mesolimbic system, with input from the ventral tegmental area, degenerates during the disease course, it declines to a lesser degree (MacDonald and Monchi, 2011; Alberico et al., 2015). Patients with higher D_2-like BP_{ND} in the hippocampus and amygdala may have better preserved ventral tegmental area to mesial temporal dopamine networks, accounting for their superior inhibitory control. We consider that in healthy dopaminergic circuits, D_2-type dopamine receptors in the dorsal striatum serve as critical modulators of response inhibition. It is possible that nigrostriatal degeneration unmasks relationships between motor action control and mesolimbic dopamine. Alternatively, these relationships may indicate a compensatory mechanism, with PD patients developing a greater reliance on limbic dopamine networks to regulate action control. The results align with previous findings of comparatively conserved dopaminergic mesolimbic networks and faster SSRTs in patients with ICBs (Claassen et al., 2015; Stark et al., 2018a).

Dopamine and the limbic cortex in PD

These results highlight a novel relationship between hippocampal and limbic regulation of action control, emphasizing previous anatomic findings that the limbic and motor loops are functionally connected. Notably, a recent study in rodents proposed that these two circuits are linked in a single direction, such that the limbic ventral striatum regulates primary motor cortex function (Aoki et al., 2019). Rather than adopting the standard notion that limbic and sensorimotor information are processed in parallel, Aoki and colleagues introduce an open cortico-basal ganglia loop. According to this interpretation, the ventral striatum, which receives inputs from the ventral tegmental area, amygdala, ventromedial prefrontal cortex, and orbitofrontal cortex, is able to inhibit substantia nigra neurons projecting to the motor thalamus (Choi et al., 2017; Aoki et al., 2019). Our data appear to illustrate an important translational example of limbic regulation of motor control through the amygdala and hippocampus in humans.

Amphetamine effects on action control

The results of this study reflect the notion that persons with PD experience differential effects to dAMPH with respect to their

Table 3. [^{18}F]Fallypride BP_{ND} (baseline) effects on SSRT

ROI	[^{18}F]fallypride BP_{ND} Mean ± SD	SSRT ~ BP_{ND} + age + sex 95% CI	Coefficient	*p* value[a]
Ventral striatum	15.15 ± 2.68	[−15.131, 2.478]	−6.33	0.145
Caudate	16.69 ± 2.35	[−16.140, 5.264]	−5.44	0.292
Putamen	22.37 ± 3.55	[−9.766, 6.030]	−1.87	0.618
Substantia nigra	1.23 ± 0.26	[−132.333, 5.466]	−63.43	0.068
Globus pallidus	10.14 ± 1.84	[−16.358, 7.822]	−4.27	0.459
Amygdala	2.18 ± 0.54	[−78.796, −17.734]	−48.26	0.005[b]
Hypothalamus	2.64 ± 0.43	[−96.176, 18.600]	−38.79	0.168
Thalamus	1.75 ± 0.37	[−103.651, 20.669]	−41.49	0.173
Hippocampus	0.98 ± 0.27	[−175.101, −34.775]	−104.94	0.007[b]
Insula	2.13 ± 0.79	[−38.278, 22.924]	−7.68	0.597
Ventromedial orbitofrontal Cortex	4.16 ± 1.73	[−21.157, 2.239]	−9.46	0.104
Anterior cingulate cortex	0.20 ± 0.12	[−266.992, 45.958]	−110.52	0.151

GLM with FDR controlled at 0.05 to correct for multiple comparisons.
[a] Uncorrected *p* value.
[b] Significant *p* value at FDR = 0.05.

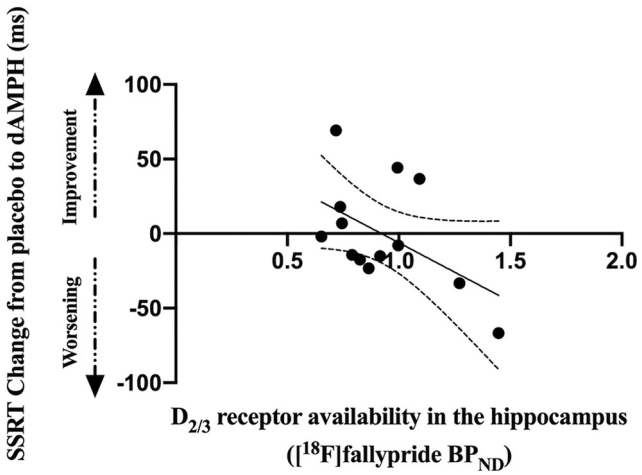

Figure 4. Scatterplot with line of best fit displaying the relationship between SSRT change (SSRT placebo − SSRT dAMPH) and baseline [^{18}F]fallypride BP_{ND}. A GLM was applied with SSRT change as the dependent variable and mean ROI BP_{ND} as the independent variable. Age and sex served as covariates. A negative correlation between BP_{ND} and SSRT change was observed for the hippocampus ($p = 0.045$), but it did not survive FDR correction for multiple comparisons at 0.05.

performance on the stop-signal task. As seen in Figure 4, some demonstrate improvement (positive SSRT change) and reduced SSRT, while others do not.

Previous work has likewise shown conflicting effects of dAMPH on SSRT performance. Various rodent studies have illustrated dose-dependent and baseline-dependent SSRT changes with amphetamine (Feola et al., 2000; Eagle and Robbins, 2003; Eagle et al., 2007). Furthermore, studies with healthy volunteers have seen similar conditional results (de Wit et al., 2000; Dolder et al., 2018). Doses of 5, 10, and 20 mg of dAMPH, used by Weafer and de Wit, significantly reduced SSRT, implying that low to moderate doses can modulate action control (Weafer and de Wit, 2013). A consistent theme is that dAMPH appears to improve performance in participants with longer baseline SSRTs (Feola et al., 2000; Weafer and de Wit, 2013). Similar results are observed with this clinical population, implying that PD patients may reach an optimal level of performance, after which a stimulant is ineffectual.

When examining the effect of dAMPH on stop-signal task performance, greater hippocampal D_2-like BP_{ND} is associated with more negative SSRT change (worse performance with dAMPH). It is likely that the positive influence of D_2-like BP_{ND} on action control, as previously discussed, acts on hippocampal networks. Previous studies investigating the effect of dopamine on working memory have suggested an inverted-U shaped role for exogenous dopamine (Cools and D'Esposito, 2011). This model indicates that at optimal baseline working memory, additional dopamine would only worsen performance. Similarly, we see that patients with greater D_2-like BP_{ND} in the hippocampus and amygdala have already attained their best SSRTs and cannot see further improvement with dAMPH. Conversely, dAMPH appears to be rescuing poor stop-signal task performance and improving SSRTs. The clinical implication of such dopaminergic actions suggests that as dAMPH alters monoamine levels, the stimulant is more likely to benefit patients with slow baseline SSRTs.

Our discovery of relationships between D_2-like BP_{ND} and placebo SSRT, along with SSRT change, emphasizes a role of D_2-like receptors in the hippocampus and amygdala on action-control. Previous studies have suggested that dopaminergic communication in the hippocampus bolsters stimulus generalization, as D_2 receptor-blockade has been shown to modulate similarity processing in humans (Kahnt and Tobler, 2016). While the stop-signal paradigm is not implemented as a reward task, participants may perceive and, accordingly, respond to the color-changing arrows with varying degrees of discrimination. Moreover, there is increasing support for the idea that the hippocampus is involved in visual perception, in addition to its established implication in memory (Lee et al., 2012). Although the response inhibition task has not been considered in terms of spatial perception, the configuration of directional stimuli is undoubtedly spatial in nature, and thus may in fact prompt hippocampal involvement. Research into the function of D_2 receptors in the amygdala is consistent with our data, as rodent experiments have concluded that D_2 expression in the central nucleus of the amygdala regulates impulsive behavior (Kim et al., 2018). As our results highlight both the hippocampus and amygdala, it is prudent to try to disentangle their respective roles in accordance with the stop-signal task. Over the course of the paradigm, it is likely that participants may begin to predict the incidence of a stop-signal, and may even consider "go" as a rewarding or positive stimulus and "stop" as a punishing or negative stimulus. In this case, the amygdala may function to learn

and process reward for impulsivity, while the hippocampus may serve to discriminate and generalize between stimuli.

In conclusion, although this study benefitted from the ability to gather behavioral information on both placebo and dAMPH, it is possible that the stop-signal task was conducted too soon after dAMPH administration. By assessing inhibition early in the context of dAMPH exposure, we may not have assessed the true effect of increased dopamine on SSRT. Future work should try to mitigate this by implementing a delay of ~2 h between drug administration and behavioral testing (Fillmore et al., 2005).

Furthermore, the apparent effects of dAMPH on inhibitory control may not be dopaminergic in nature. While dAMPH predominantly acts by communicating with dopamine neurons, it nevertheless is capable of interacting with other neurotransmitters, including serotonin, acetylcholine, and norepinephrine (Moore, 1977). In light of this, the inference that dopamine is the main contributor to these results must be made with a caveat that other monoamines acting on hippocampal and amygdala regions may modulate action control in humans. Finally, we acknowledge the limitations of a small sample size, given the arduous PET and dAMPH methods, and are optimistic that future studies with larger patient bases will further substantiate and build on this work.

References

Ahlskog JE (2010) Think before you leap: donepezil reduces falls? Neurology 75:1226–1227.

Alberico SL, Cassell MD, Narayanan NS (2015) The vulnerable ventral tegmental area in Parkinson's disease. Basal Ganglia 5:51–55.

Aoki S, Smith JB, Li H, Yan X, Igarashi M, Coulon P, Wickens JR, Ruigrok TJH, Jin X (2019) An open cortico-basal ganglia loop allows limbic control over motor output via the nigrothalamic pathway. Elife 8:e49995.

Aumann MA, Stark AJ, Hughes SB, Lin YC, Kang H, Bradley E, Zald DH, Claassen DO (2020) Self-reported rates of impulsivity in Parkinson's disease. Ann Clin Transl Neurol 7:437–448.

Bechara A, Damasio H, Damasio AR (2000) Emotion, decision making and the orbitofrontal cortex. Cereb Cortex 10:295–307.

Benjamini Y, Hochberg Y (1995) Controlling the false discovery rate: a practical and powerful approach to multiple testing. J R Stat Soc Series B Stat Methodol 57:289–300.

Björklund A, Dunnett SB (2007) Dopamine neuron systems in the brain: an update. Trends Neurosci 30:194–202.

Camps M, Cortés R, Gueye B, Probst A, Palacios JM (1989) Dopamine receptors in human brain: autoradiographic distribution of D2 sites. Neuroscience 28:275–290.

Choi EY, Ding SL, Haber SN (2017) Combinatorial inputs to the ventral striatum from the temporal cortex, frontal cortex, and amygdala: implications for segmenting the striatum. eNeuro 4:ENEURO.0392-17.2017.

Claassen DO, van den Wildenberg WPM, Harrison MB, van Wouwe NC, Kanoff K, Neimat JS, Wylie SA (2015) Proficient motor impulse control in Parkinson disease patients with impulsive and compulsive behaviors. Pharmacol Biochem Behav 129:19–25.

Colzato LS, van Wildenberg WPM, Hommel B (2007) Impaired inhibitory control in recreational cocaine users. PLoS One 2:e1143.

Colzato LS, van den Wildenberg WPM, van Wouwe NC, Pannebakker MM, Hommel B (2009) Dopamine and inhibitory action control: evidence from spontaneous eye blink rates. Exp Brain Res 196:467–474.

Cools R, D'Esposito M (2011) Inverted-U shaped dopamine actions on human working memory and cognitive control. Biol Psychiatry 69:e113–e125.

Damier P, Hirsch EC, Agid Y, Graybiel AM (1999) The substantia nigra of the human brain. II. Patterns of loss of dopamine-containing neurons in Parkinson's disease. Brain 122:1437–1448.

de Wit H, Crean J, Richards JB (2000) Effects of d-amphetamine and ethanol on a measure of behavioral inhibition in humans. Behav Neurosci 114:830–837.

Dolder PC, Strajhar P, Vizeli P, Odermatt A, Liechti ME (2018) Acute effects of lisdexamfetamine and D-amphetamine on social cognition and cognitive performance in a placebo-controlled study in healthy subjects. Psychopharmacology (Berl) 235:1389–1402.

Eagle DM, Robbins TW (2003) Lesions of the medial prefrontal cortex or nucleus accumbens core do not impair inhibitory control in rats performing a stop-signal reaction time task. Behav Brain Res 146:131–144.

Eagle DM, Tufft MRA, Goodchild HL, Robbins TW (2007) Differential effects of modafinil and methylphenidate on stop-signal reaction time task performance in the rat, and interactions with the dopamine receptor antagonist cis-flupenthixol. Psychopharmacology (Berl) 192:193–206.

Eagle DM, Wong JCK, Allan ME, Mar AC, Theobald DE, Robbins TW (2011) Contrasting roles for dopamine D1 and D2 receptor subtypes in the dorsomedial striatum but not the nucleus accumbens core during behavioral inhibition in the stop-signal task. J Neurosci 31:7349–7356.

Enticott PG, Ogloff JRP, Bradshaw JL (2008) Response inhibition and impulsivity in schizophrenia. Psychiatry Res 157:251–254.

Feola TW, de Wit H, Richards JB (2000) Effects of d-amphetamine and alcohol on a measure of behavioral inhibition in rats. Behav Neurosci 114:838–848.

Fillmore MT, Kelly TH, Martin CA (2005) Effects of d-amphetamine in human models of information processing and inhibitory control. Drug Alcohol Depend 77:151–159.

Ghahremani DG, Lee B, Robertson CL, Tabibnia G, Morgan AT, De Shetler N, Brown AK, Monterosso JR, Aron AR, Mandelkern MA, Poldrack RA, London ED (2012) Striatal dopamine D2/D3 receptors mediate response inhibition and related activity in frontostriatal neural circuitry in humans. J Neurosci 32:7316–7324.

Goetz CG, Tilley BC, Shaftman SR, Stebbins GT, Fahn S, Martinez-Martin P, Poewe W, Sampaio C, Stern MB, Dodel R, Dubois B, Holloway R, Jankovic J, Kulisevsky J, Lang AE, Lees A, Leurgans S, LeWitt PA, Nyenhuis D, Olanow CW, et al. (2008) Movement disorder society-sponsored revision of the unified Parkinson's disease rating scale (MDS-UPDRS): scale presentation and clinimetric testing results. Mov Disord 23:2129–2170.

Hughes AJ, Daniel SE, Kilford L, Lees AJ (1992) Accuracy of clinical diagnosis of idiopathic Parkinson's disease: a clinico-pathological study of 100 cases. J Neurol Neurosurg Psychiatry 55:181–184.

Kahnt T, Tobler PN (2016) Dopamine regulates stimulus generalization in the human hippocampus. Elife 5:e12678.

Kim B, Yoon S, Nakajima R, Lee HJ, Lim HJ, Lee YK, Choi JS, Yoon BJ, Augustine G, Baik JH (2018) Dopamine D2 receptor-mediated circuit from the central amygdala to the bed nucleus of the stria terminalis regulates impulsive behavior. Proc Natl Acad Sci USA 115:E10730–E10739.

Klomp A, Koolschijn PCMP, Hulshoff Pol HE, Kahn RS, Haren NEMV (2012) Hypothalamus and pituitary volume in schizophrenia: a structural MRI study. Int J Neuropsychopharmacol 15:281–288.

Lee ACH, Yeung LK, Barense MD (2012) The hippocampus and visual perception. Front Hum Neurosci 6:91.

Levitt H (1971) Transformed up-down methods in psychoacoustics. J Acoust Soc Am 49:467–477.

Logan GD, Cowan WB (1984) On the ability to inhibit thought and action: a theory of an act of control. Psychol Rev 91:295–327.

MacDonald PA, Monchi O (2011) Differential effects of dopaminergic therapies on dorsal and ventral striatum in Parkinson's disease: implications for cognitive function. Parkinsons Dis 2011:572743.

Mackey S, Petrides M (2009) Architectonic mapping of the medial region of the human orbitofrontal cortex by density profiles. Neuroscience 159:1089–1107.

Martinez-Martin P, Rodriguez-Blazquez C, Kurtis MM, Chaudhuri KR; NMSS Validation Group (2011) The impact of non-motor symptoms on health-related quality of life of patients with Parkinson's disease. Mov Disord 26:399–406.

Matzke D, Love J, Wiecki TV, Brown SD, Logan GD, Wagenmakers EJ (2013) Release the BEESTS: Bayesian estimation of ex-Gaussian STop-signal reaction time distributions. Front Psychol 4:918.

Matzke D, Love J, Heathcote A (2017) A Bayesian approach for estimating the probability of trigger failures in the stop-signal paradigm. Behav Res Methods 49:267–281.

Mink JW (1996) The basal ganglia: focused selection and inhibition of competing motor programs. Prog Neurobiol 50:381–425.

Moeller FG, Barratt ES, Dougherty DM, Schmitz JM, Swann AC (2001) Psychiatric aspects of impulsivity. Am J Psychiatry 158:1783–1793.

Moore KE (1977) The actions of amphetamine on neurotransmitters: a brief review. Biol Psychiatry 12:451–462.

Mukherjee J, Christian BT, Dunigan KA, Shi B, Narayanan TK, Satter M, Mantil J (2002) Brain imaging of 18F-fallypride in normal volunteers: blood analysis, distribution, test-retest studies, and preliminary assessment of sensitivity to aging effects on dopamine D-2/D-3 receptors. Synapse 46:170–188.

Petersen K, Van Wouwe N, Stark A, Lin YC, Kang H, Trujillo-Diaz P, Kessler R, Zald D, Donahue MJ, Claassen DO (2018) Ventral striatal network connectivity reflects reward learning and behavior in patients with Parkinson's disease. Hum Brain Mapp 39:509–521.

Pohjalainen T, Rinne JO, Någren K, Syvälahti E, Hietala J (1998) Sex differences in the striatal dopamine D2 receptor binding characteristics in vivo. Am J Psychiatry 155:768–773.

Ray NJ, Miyasaki JM, Zurowski M, Ko JH, Cho SS, Pellecchia G, Antonelli F, Houle S, Lang AE, Strafella AP (2012) Extrastriatal dopaminergic abnormalities of DA homeostasis in Parkinson's patients with medication-induced pathological gambling: a [11C] FLB-457 and PET study. Neurobiol Dis 48:519–525.

Robertson CL, Ishibashi K, Mandelkern MA, Brown AK, Ghahremani DG, Sabb F, Bilder R, Cannon T, Borg J, London ED (2015) Striatal D1- and D2-type dopamine receptors are linked to motor response inhibition in human subjects. J Neurosci 35:5990–5997.

Stark AJ, Smith CT, Lin YC, Petersen KJ, Trujillo P, van Wouwe NC, Kang H, Donahue MJ, Kessler RM, Zald DH, Claassen DO (2018a) Nigrostriatal and mesolimbic D2/3 receptor expression in Parkinson's disease patients with compulsive and reward-driven behaviors. J Neurosci 38:3230–3239.

Stark AJ, Smith CT, Petersen KJ, Trujillo P, van Wouwe NC, Donahue MJ, Kessler RM, Deutch AY, Zald DH, Claassen DO (2018b) [18F]fallypride characterization of striatal and extrastriatal D2/3 receptors in Parkinson's disease. Neuroimage Clin 18:433–442.

Tomlinson CL, Stowe R, Patel S, Rick C, Gray R, Clarke CE (2010) Systematic review of levodopa dose equivalency reporting in Parkinson's disease. Mov Disord 25:2649–2653.

Trujillo P, van Wouwe NC, Lin YC, Stark AJ, Petersen KJ, Kang H, Zald DH, Donahue MJ, Claassen DO (2019) Dopamine effects on frontal cortical blood flow and motor inhibition in Parkinson's disease. Cortex 115:99–111.

Voon V, Hassan K, Zurowski M, de Souza M, Thomsen T, Fox S, Lang AE, Miyasaki J (2006) Prevalence of repetitive and reward-seeking behaviors in Parkinson disease. Neurology 67:1254–1257.

Weafer J, de Wit H (2013) Inattention, impulsive action, and subjective response to d-amphetamine. Drug Alcohol Depend 133:127–133.

Weintraub D, Koester J, Potenza MN, Siderowf AD, Stacy M, Voon V, Whetteckey J, Wunderlich GR, Lang AE (2010) Impulse control disorders in Parkinson disease: a cross sectional study of 3090 patients. Arch Neurol 67:589–595.

Weintraub D, Mamikonyan E, Papay K, Shea JA, Xie SX, Siderowf A (2012) Questionnaire for impulsive–compulsive disorders in Parkinson's disease-rating scale. Mov Disord 27:242–247.